JOURNAL OF AIRCRAFT
Vol. 34, No. 4, July–August 1997

Computation of Cavity Flows with Suppression Using Jet Blowing

Alison M. Lamp* and Ndaona Chokani†
North Carolina State University, Raleigh, North Carolina 27695-7910

A computational investigation of a compressible cavity flow was conducted. Blowing was implemented to suppress the large pressure oscillations characteristic of cavity flows. The cavity length-to-depth ratio was 4.33, and the freestream Mach number was 1.75. A two-dimensional, time-accurate Navier–Stokes scheme was used to simulate the flow. A small jet placed within the cavity just below the front lip was used to force the shear layer with different amplitudes and frequencies. This control technique was successful in reducing the amplitude of the oscillations. Furthermore, the effectiveness of the control was found to depend upon the jet frequency, amplitude, phase angle, and duty cycle. Autocorrelation analysis showed that the jet decreased the size of the structures in the shear layer. Cross-correlation analysis showed that the timing of events within the cavity were unaffected by the jet blowing.

Introduction

CAVITY flows occur in a variety of situations where an orifice is exposed to moving fluid. Under certain conditions, intense, unsteady acoustic oscillations are produced within the cavity. These oscillations can be severe enough to damage stores in an exposed weapons bay.[1] Other problems associated with cavity flows are excessive noise from the wheel wells[2] and an increase in aerodynamic excrescence drag.[3] The severity of the problems associated with cavity flows has motivated many computational and experimental studies. These studies have been directed toward improving our understanding of the nature of cavity flows and means to control cavity flows.

There are two basic types of cavity flow, depending upon the cavity length-to-depth (L/D) ratio. For L/D ratios greater than 10, the flow is termed a closed cavity flow and is quite steady. In the applications described earlier, the L/D ratio is less than 10; in this case the flow is termed an open cavity flow and is unsteady. This flow unsteadiness arises because of the coupling of instabilities in the shear layer and acoustic disturbances within the cavity[4] (Fig. 1). The Kelvin–Helmholtz-type instabilities originate near the upstream separation point of the shear layer. These instabilities or vortices grow as they are convected downstream in the shear layer. At the downstream cavity wall, acoustic disturbances are generated as a result of the impingement of the vortices on the wall. These disturbances radiate throughout the cavity, and at the receptivity site on the upstream cavity wall they produce additional instabilities in the shear layer. A feedback loop is thus formed by the shear layer's instabilities and the cavity's acoustic disturbances. Furthermore, the interaction of the disturbances and the shear layer produces large vertical displacements of the shear layer as it bridges the cavity opening; these displacements result in a mass and momentum exchange, which is most marked at the cavity downstream wall. These aforementioned phenomena produce the undesirable cavity flow oscillations that are encountered in the practical applications.

A number of different methods have been developed to suppress the cavity oscillations. One class of suppression techniques used is passive control. In this approach, the cavity is modified in some way, usually with mounted devices. Some examples of these are spoilers[5,6] and trailing-edge slants[5,7] that modify the shear layer, and cowls[5] that interrupt the mass transfer above the cavity downstream wall. Passive pneumatic control, whereby the pressure difference in the cavity is exploited to transport fluid along the cavity floor, has been examined by Chokani and Kim.[8] Passive control methods have been found to be inexpensive, simple, and at certain flow conditions, very effective in suppressing the cavity oscillations. However, since the passive control uses permanent devices, the performance of the cavity at off-design or in time-varying conditions may actually be worse than the performance of a cavity without passive control.

Active control methods, on the other hand, can continuously change to adapt to different flow conditions. Vakili et al.[9] injected fluid upstream of the cavity to modify the shear layer. The cavity dynamics were significantly altered, and a 27 dB decrease in the peak pressure amplitude was measured. Sarno and Franke[10] conducted experiments using a small fence or a small jet at the upstream cavity wall. They found that a pulsing jet could be used to decrease the peak pressure amplitude by up to 8 dB. These studies were useful in that the feasibility of an active control method was demonstrated. However, in the absence of detailed measurements, it is difficult to discern the nature of the control mechanism. The advent of high-performance computer hardware, miniaturized actuators and sensors, and microelectromechanical systems has renewed interest in active flow systems. The previous high-cost, heavy weight, and unreliability are no longer pacing factors in the implementation of active control systems. The potential does exist for the improved control of cavity oscillations under a wide range of conditions. The primary objective of the present work is to demonstrate the capability of state-of-the-art computational fluid dynamics methods to simulate blowing control of a compressible, unsteady, separated flow that then could be implemented in an active control system.

The approach taken in the present work was to perform time-accurate Navier–Stokes simulations of the compressible flow past a cavity with and without blowing control. The two-dimensional Navier–Stokes code developed by Morgenstern and Chokani[11] was used for this purpose. This code has pre-

Presented as Paper 96-0446 at the AIAA 34th Aerospace Sciences Meeting, Reno, NV, Jan. 15–18, 1996; received June 3, 1996; revision received Feb. 28, 1997; accepted for publication March 5, 1997.

*Graduate Student, Department of Mechanical and Aerospace Engineering. Student Member AIAA.

†Associate Professor, Department of Mechanical and Aerospace Engineering. Senior Member AIAA.

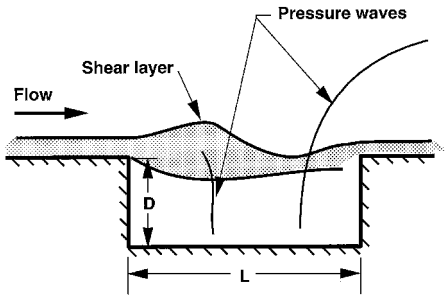

Fig. 1 Open cavity flow.

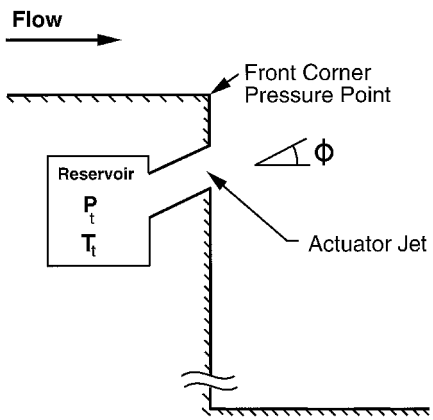

Fig. 2 Schematic figure of jet placement within the cavity.

viously been shown to accurately capture the unsteady characteristics of cavity flows. Turbulence closure was accomplished through the use of an algebraic eddy viscosity model. The same turbulence model was used for the computations with and without blowing control. The turbulence model inadequacies in the prediction of the effects of the fine-scale turbulence are limited to the components of the frequency spectra at values much higher than those associated with the cavity flow's unsteadiness. Thus, in the present work, where the focus is on the effectiveness of the control technique, the simple turbulence model is deemed adequate. The computationally efficient code is thus used to conduct detailed parametric studies of the active control of compressible cavity flows.

The blowing control used in this study consisted of a small steady or pulsing jet placed within the cavity below the front lip (Fig. 2). The present study examines the following issues: what are the effects of the jet on the cavity flow dynamics, and how effective is this technique in attenuating the oscillations? In the next section, the numerical code and the spectral analysis techniques are described. Some details of the cavity dynamics are then presented in the Results and Discussion section. The spectral analysis for the baseline case without blowing, for the steady blowing jets, and for the pulsing jets are also presented. Finally, the conclusions concerning the effectiveness of the blowing control using the jet are presented.

Numerical Techniques

Unsteady, two-dimensional calculations of the cavity flowfields were conducted using the implicit, Navier–Stokes solver developed by Morgenstern and Chokani.[11] The code is used to solve the unsteady, compressible, turbulent flows on finite volume grids. The Baldwin–Lomax turbulence model, modified for cavity flows, is used to model the effects of fine-scale turbulence.[12] An implicit algorithm based on the lower-upper, symmetric-Gauss–Seidel (LU–SGS) scheme with a Newton subiteration procedure is used to perform the time-accurate calculations of the unsteady flows. The Newton subiteration procedure is employed to eliminate the linearization and factorization errors of the basic LU–SGS scheme. The implicit algorithm yields results that are temporally and spatially accurate to the second order. A multiblock approach is used in the calculations to efficiently utilize the computer memory. East[13] and Rizzetta[14] have shown that the cavity flow phenomena are largely two dimensional in character. Thus, in the present work, a two-dimensional study is conducted.

The implementation of the jet boundary conditions are described in detail in Ref. 15, but a few salient features are presented here. The jet is placed just beneath the upstream cavity wall lip (Fig. 2). The jet opening is $0.045D$, and its top is located $0.018D$ below the lip. The three parameters specified for the jet are 1) injection angle ϕ, 2) total pressure P_t, and 3) total temperature T_t. For the pulsing jets, a phase angle θ, peak-to-peak amplitude, and pulsing frequency f of the total pressure are also specified. For all cases presented here, $\theta = 45$ deg and $T_t = 298$ K. The jet was choked for all of the cases examined; therefore, the jet exit pressure and temperature are calculated using the isentropic relations. The jet exit velocity is then calculated using the jet exit temperature. A uniform velocity, pressure, and temperature profile is assumed across the jet opening.

Table 1 Comparison of computational and experimental cavity resonant frequencies with the Rossiter formula predictions

Mode	Present work	Vakili et al.[9]	Rossiter, Eq. (1)
First	719 (12%)	830 (29%)	640
Second	1496 (−.1%)	1592 (6.5%)	1494
Third	2259 (−3.8%)	2540 (8.1%)	2348

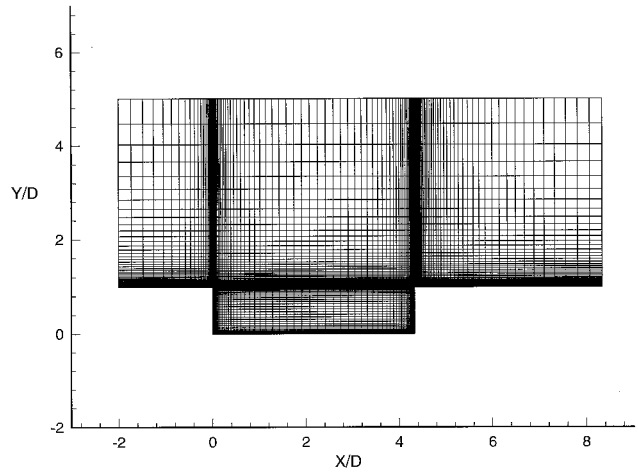

Fig. 3 Computational grid for the cavity, $L/D = 4.33$.

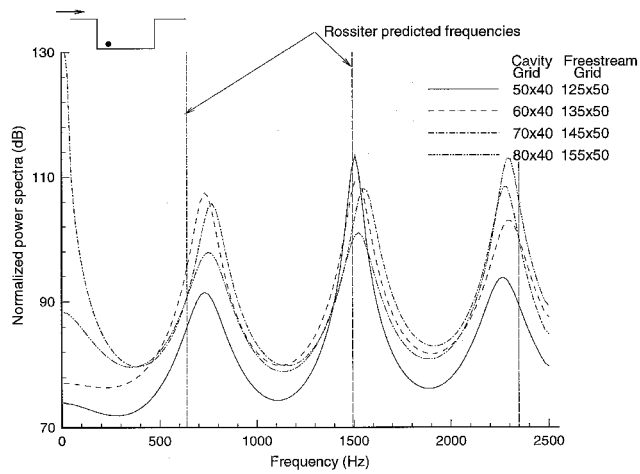

Fig. 4 Comparison of grid refinement spectra with Rossiter formula prediction.

Table 2 Summary of test cases examined[a]

Case	P_r, kPa	m, kg/s	Duty cycle	f, Hz	θ, deg
1	213	0.021	Steady	——	——
2	450	0.044	Steady	——	——
3	213	0.010	Square	711	0
4	213	0.010	Square	711	180
5	213	0.021	Sinusoid[b]	711	0
6	213	0.021	Sinusoid[b]	500	180
7	450	0.044	Sinusoid[b]	500	0
8	450	0.044	Sinusoid[b]	500	180
9	450	0.044	Sinusoid[b]	1000	0
10	55.5	0.035	Steady, distributed upstream blowing		

[a]$M_\infty = 1.75$, $Re = 5.58 \times 10^7$/m. [b]Peak-to-peak amplitude is 94.5 kPa.

These calculated exit values are used to determine the ghost cell values for the finite volume mesh.

Spectra of the cavity pressures were obtained using the maximum entropy method (MEM) for spectral estimation.[12,16] In comparison to the more traditional fast Fourier transform approach, the MEM makes no assumptions about the data, nor are the data artificially manipulated. However, the MEM yields a power spectrum density estimate given as

$$S(f) = \frac{P_m \Delta t}{\left| 1 - \sum_{n=1}^{m} a_{mn} \exp(-2\pi j f n \Delta t) \right|^2}$$

where P_m is the output power associated with the $(m + 1)$ length predictor–error filter; a_{mn} are the filter coefficients; and Δt is the time interval of the equally spaced data samples. This MEM spectrum is integrated over the frequency bandwidth to obtain the power spectrum (a reference pressure of 2×10^{-5} Pa is used to normalize the cavity pressures).

The semiempirical formula, developed by Rossiter,[6] and modified by Heller and Bliss[5] for compressible flows, was used to predict the cavity resonant frequencies. The modified formula is

$$f_m = \frac{U_\infty}{L} \frac{m - \alpha}{\dfrac{M_\infty}{\sqrt{1 + [(\gamma - 1)/2] M_\infty^2}} + \dfrac{1}{k_v}} \tag{1}$$

where γ is the ratio of specific heats; M_∞ and U_∞ are the freestream Mach number and flow speed, respectively; and f_m is the resonant frequency corresponding to the mth mode. Heller and Bliss[5] determined from their experiments that the constants α and k_v are 0.25 and 0.57, respectively. Heller et al.[17] estimated that for cavities with a L/D ratio of 4 or more, the difference between the Rossiter formula and experiments should be within ±10%.

Results and Discussion

For purposes of comparison, the present study was conducted using the same test conditions Vakili et al.[9] used in their upstream blowing experiments. The freestream Mach number was 1.75, stagnation pressure 310 kPa, and unit Reynolds number 5.58×10^7/m. The total temperature was 256 K and an adiabatic wall is assumed. The computational grid for the cavity with L/D ratio of 4.33 used in this study is shown in Fig. 3. In the streamwise and streamwise-normal $(X \times Y)$ directions, this grid contained 70×40 and 145×50 points in the cavity and freestream regions, respectively. The points were clustered along the walls and the expected shear-layer region between the cavity and the freestream to resolve the free shear layer and the boundary layer. The boundary layer upstream of the cavity contained 22 streamwise-normal points. A grid refinement study was conducted to ensure that the results were independent of the grid dimensions. For all four grids examined (50×40 and 125×50, 60×40 and 135×50, 70×40 and 145×50, and 80×40 and 155×50), the spectra calculated using the MEM basically show the same spectral characteristics (Fig. 4). The vertical lines represent the modified Rossiter formula predictions. In the insert figure, the filled symbol shows the location of the data sampling point. In all the spectral analysis, 50 averages of data records each containing 174 points were used. The resultant spectral resolution was 19.4 Hz.

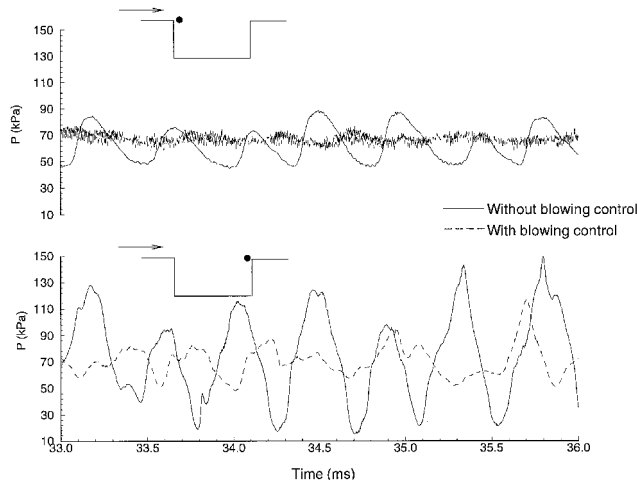

Fig. 5 Comparison of the pressure–time histories with and without blowing control at the front and back lip locations.

Table 1 compares the spectral frequencies of the computation, the baseline experiment of Vakili et al.,[9] and the Rossiter formula, Eq. (1). The values in parentheses are the percent difference compared with the Rossiter prediction. Only the first three modes are shown. The computational data are within the difference Heller et al.[17] estimated. The experimental data of Vakili et al.[9] also compare well, with the exception of the first mode.

The mass flow rates m and description of the different blowing control test cases examined in this study are given in Table 2. A typical run on a Cray Y-MP supercomputer required approximately 4 CPU hours.

Cavity Dynamics

Pressure–time traces at the front and back lip locations of the cavity illustrate features of the cavity dynamics. Figure 5 compares the pressure–time traces of the cavity without control (baseline case) and a representative case with control (case 9). The cavity without control shows very regular flow oscillations with a large pressure variation between the two locations. With control, the amplitudes are reduced, the oscillations are irregular, and the pressure–time traces at the front lip location show little variation.

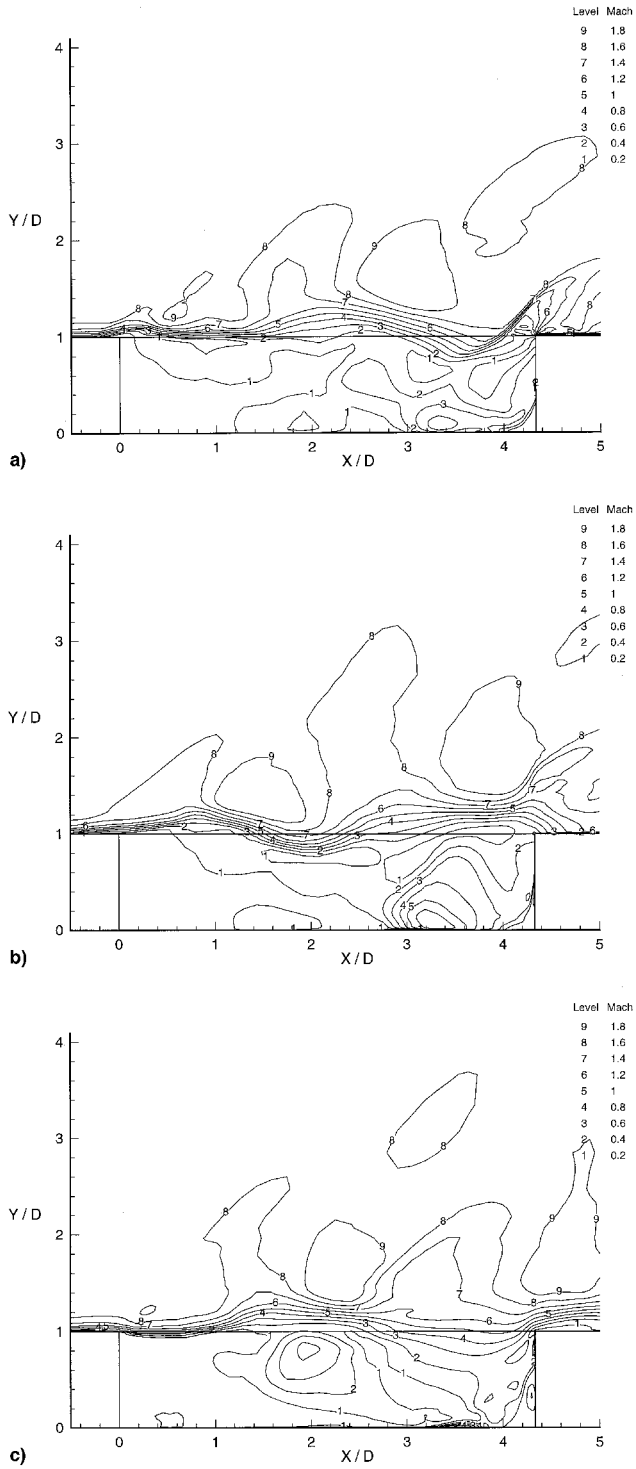

Fig. 6 Baseline cavity Mach number contours. Time = a) 34.9, b) 35.0, and c) 35.1 ms.

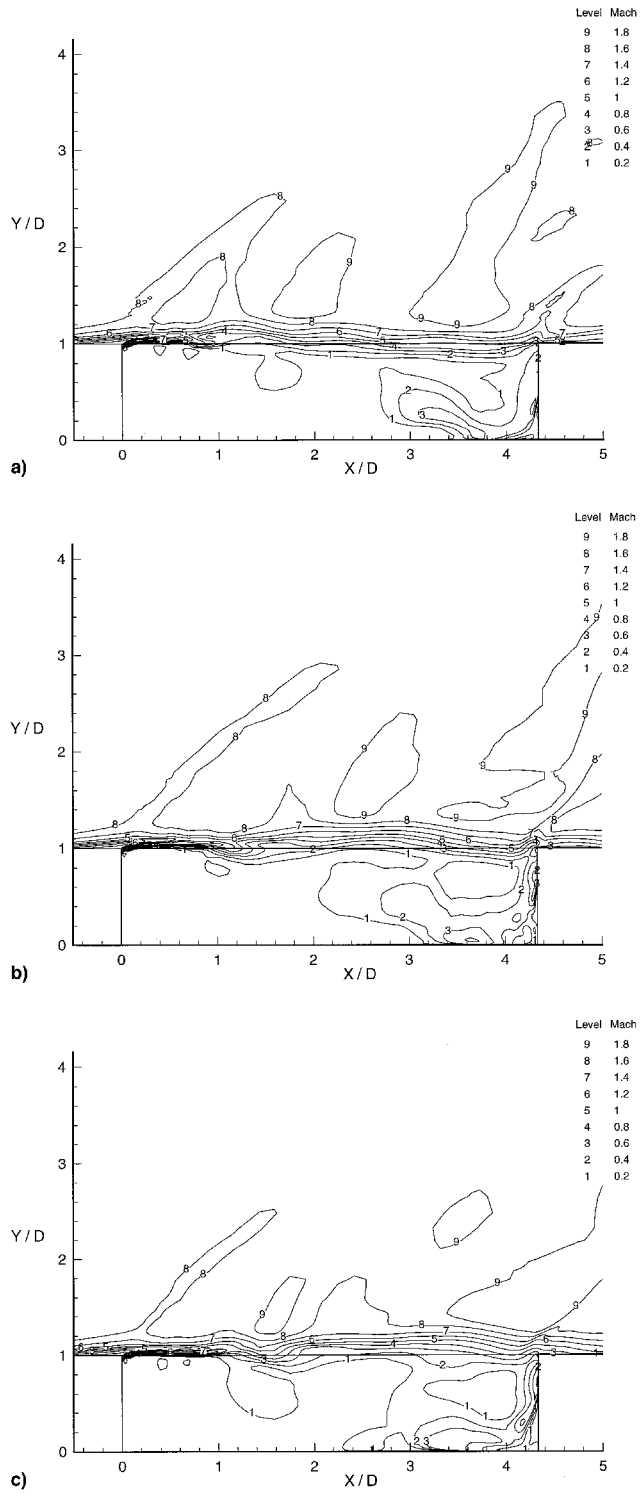

Fig. 7 Cavity Mach number contours with blowing control (case 9). Time = a) 35.0, b) 35.1, and c) 35.2 ms.

Figures 6 and 7 show a series of instantaneous Mach contours of the cavity flowfield for the baseline case and for the pulsing jet control case (case 9). The first snapshots of the series are chosen when the pressure at the back lip location is a maximum. Since the baseline case is so regular, one cycle is divided equally into three time intervals; this same interval is also used for the control cases. Figures 6a–6c illustrate the unsteadiness of the cavity flow for the baseline case. In Figure 6a, fluid is seen leaving the cavity near the back wall. The movement of a small disturbance in the shear layer near the front wall can be traced through the time series. This disturbance grows in amplitude as it progresses downstream (Figs. 6b and 6c). For the blowing control case (Fig. 7), blowing has suppressed the cavity oscillations.

Steady Blowing

Two steady blowing cases, cases 1 and 2, with total reservoir pressures of 213 and 450 kPa, respectively, were examined. The jet reservoir pressures yield jet mass flow rates comparable to those used in the Sarno and Franke[10] experiment. Power spectra of the steady blowing cases are compared to the baseline case in Fig. 8. The blowing causes a frequency shift at the first mode by 4% for the low-blowing jet case and 26%

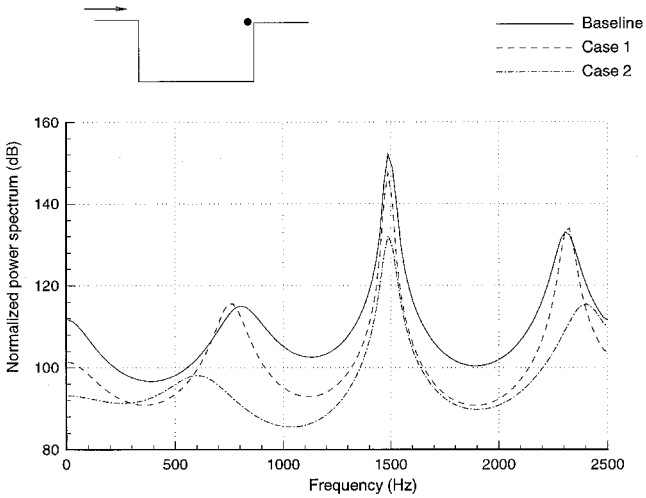

Fig. 8 Comparison of the cavity pressure power spectra using different blowing amplitudes for steady blowing control: cases 1 and 2.

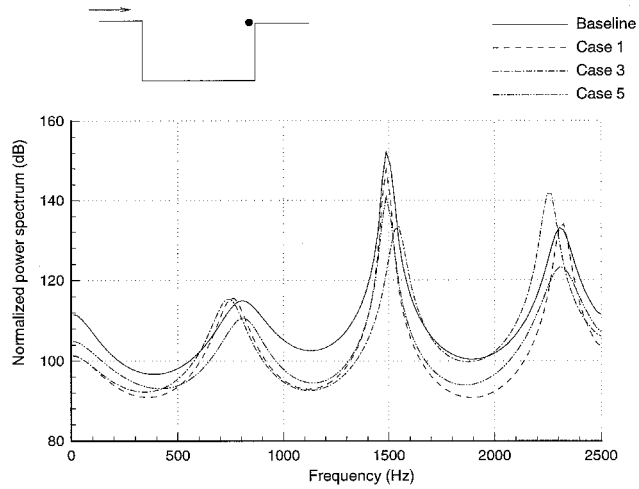

Fig. 9 Comparison of the cavity pressure power spectra using steady, square, and sinusoidal duty cycles: cases 1, 3, and 5.

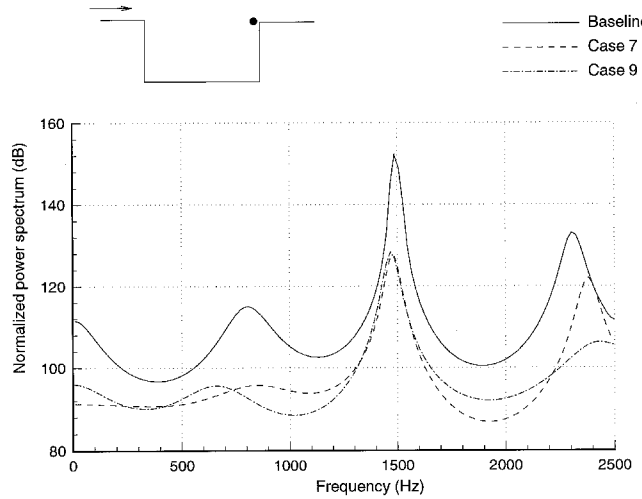

Fig. 10 Comparison of the cavity pressure power spectra at the back lip location using different pulsing frequencies: cases 7 and 9.

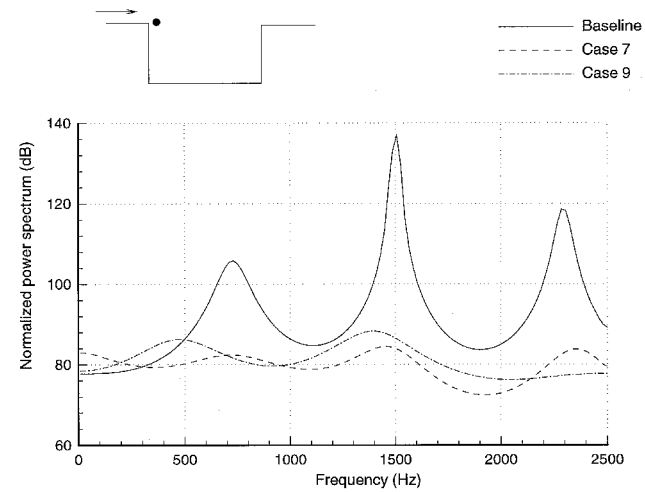

Fig. 11 Comparison of the cavity pressure power spectra at the front lip location using different pulsing frequencies: cases 7 and 9.

for the high-blowing jet case. The larger blowing rate produced the greatest reduction in amplitude across the entire spectrum. The lower blowing rate, however, shows reductions in the amplitude of the second mode, while increasing the amplitudes of the first and third modes.

Pulsing Blowing

Two duty cycles were used for the pulsing blowing: a pulsed square wave, or an on–off type action valve and a sinusoidal, continuous blowing jet. A forcing frequency of 711 Hz, the frequency of the baseline's first resonant mode at the front lip, was used. Figure 9 shows the power spectra of the two pulsed blowing jets, cases 3 and 5, compared to the steady blowing jet, case 1. The baseline case with no blowing is also shown for comparison. The pulsed square wave blowing jet (case 3) shows an increase in amplitude for the third mode and a significant reduction in the second mode. The sinusoidal duty cycle (case 5) does not increase the amplitude at the third mode unlike the square duty cycle and the steady blowing jet cases. Pulsing is seen to be more effective in suppressing the second mode compared to the steady jet.

The effects of sinusoidal pulsing at frequencies other than a resonant frequency are shown in Fig. 10. Frequencies 500 and 1000 Hz, cases 7 and 9, respectively, were chosen since they differ from the baseline cavity resonant mode frequencies and have low amplitudes in the baseline spectrum. Pulsing the jet at 1000 Hz is more effective at reducing the amplitude of the third mode. The amplitude reductions at the first and second modes are approximately the same. For both the 500- and 1000-Hz cases, there was no increase in amplitude at the pulsing frequencies. Spectra obtained from data sampled at the top corner of the cavity front wall are shown in Fig. 11 for the 500- and 1000-Hz cases. For both cases, the frequencies are considerably damped out at the front wall. Even though there is no clear evidence of the oscillations at the front wall for the 1000-Hz jet (Fig. 5), by the time the fluid in the shear layer has convected to the back wall, measurable oscillations have developed.

Figure 12 shows the effect of the pulsing jet pressure amplitude for the 500-Hz sinusoidal wave, cases 6 and 8. The steady-blowing jet cases (cases 1 and 2) are also shown for comparison. The higher pressure jet (case 8) was more effective at reducing the amplitude at all of the modes; whereas the lower pressure jet (case 6) reduces the spectral amplitudes at all but the third mode. It was previously observed that the pulsing jet was more effective than the steady blowing jet in suppressing the second mode. However, for the first mode, the low-amplitude pulsing jet is more effective than the low-amplitude steady jet. For the third mode, the pulsing high-amplitude jet is more effective than the steady blowing jet.

Figure 13 summarizes the spectral amplitude reduction in decibels between the control cases and the baseline case. For each case, the decibel reduction is shown for the first, second,

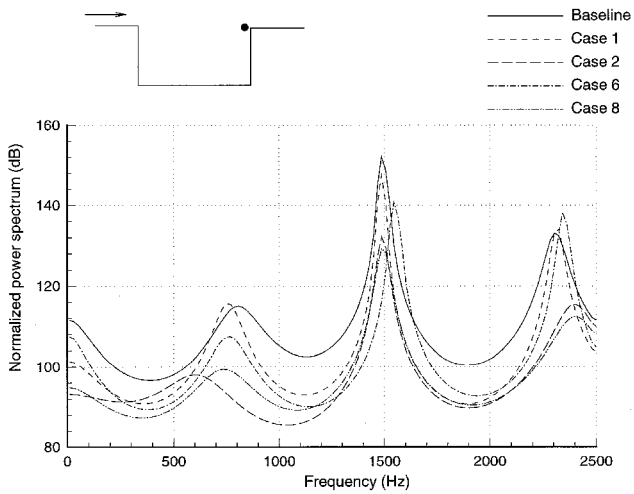

Fig. 12 Comparison of the cavity pressure power spectra using different amplitude pulsing jets: cases 1, 2, 6, and 8.

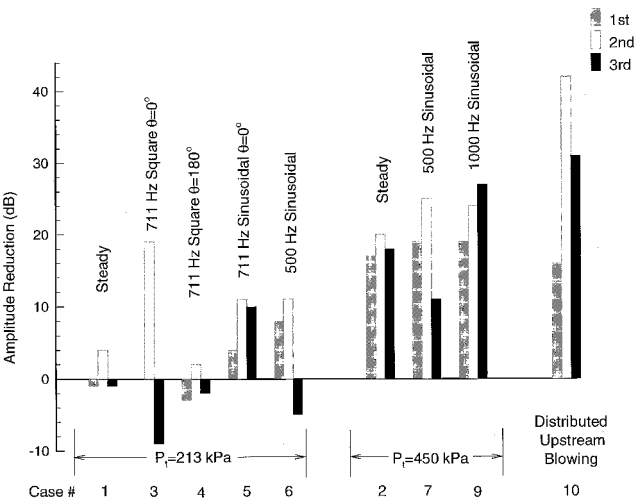

Fig. 13 Summary of cavity pressure reduction in decibels for the first three modes by different control methods.

and third modes. These cases are compared to a computational simulation of the upstream blowing experiment of Vakili et al.,[9] case 10. In the experiment, a large porous plate was located upstream of the cavity. This simulation modeled the low-density hole configuration (plate 8 in Ref. 9), with the intermediate blowing rate of 0.035 kg/s. As can be seen, the amplitude reductions using the small jet are comparable to the measured reductions of case 10 and are accomplished with comparable mass flow rates (Table 2). For the lower amplitude blowing cases (P_t = 213 kPa), the effect of the four jet parameters (phase, duty cycle, pulsing, and pulsing frequency) on the most intense resonance at the second mode can be summarized as follows. The second mode suppression is most effective at ϕ = 0 deg compared with ϕ = 180 deg. The square duty cycle yields more beneficial reductions in the second mode amplitude than the sinusoidal duty cycle; however, the sinusoidal duty cycle has a less adverse effect on the first and third modes. With the exception of the square duty cycle, ϕ = 180-deg case, the pulsing jet is seen to be more effective in the second mode suppression than the steady amplitude jet. No clear evidence of the pulsing jet's frequency is seen at this low-amplitude blowing. At the higher amplitude blowing (P_t = 450 kPa), pulsing the blowing jet is seen to be effective in suppression of all three observed resonant modes. For both the steady and pulsing jet it is seen that the suppression is more effective at the higher blowing amplitude.

Autocorrelation Analysis

Autocorrelation analysis was conducted to examine the effect of blowing on the length scales of the shear-layer instabilities. Figure 14 shows the autocorrelation coefficient taken at the back lip location for cases 1, 2, 6, 7, and 9. The autocorrelation function rolls off more quickly for all cases shown, except for the low-amplitude, steady blowing, case 1. This rolloff is indicative of the smaller scales in the shear layer. The high-amplitude blowing is more effective in reducing the length scales than the low-amplitude blowing cases. This reduction in length scales correlates with the reduction of pressure amplitude shown in Fig. 13.

Cross-Correlation Analysis

Cross-correlation analysis was used to assess the effect of the jet blowing on the timing of the cyclic disturbances within the cavity. As described by Heller and Bliss,[5] these disturbances consist of vortices that are shed at the front cavity lip and are then convected downstream, and pressure waves that arise from the impingement of the vortices at the cavity rear wall and are then propagated upstream. In the normalized cross-correlation plot, the peak amplitudes are indicative of the correlated events between the two measured stations. Figure 15 shows the normalized cross-correlation coefficient between the front lip station and back lip station for several low-amplitude blowing cases. The convection velocities may be calculated using the linear distance between the two measurement stations divided by the time lag τ. From this analysis, the peak

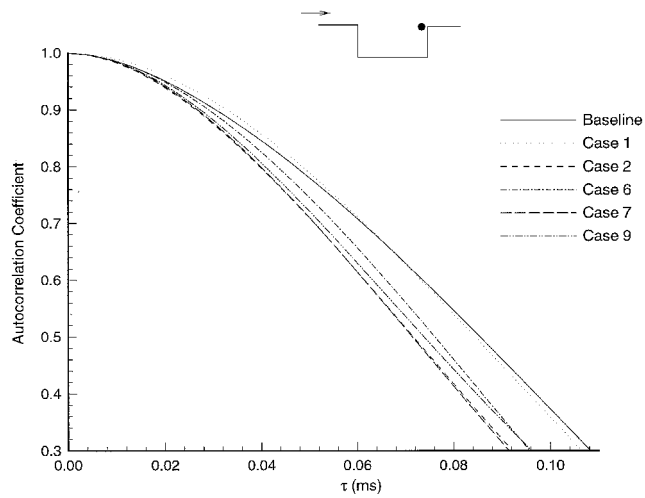

Fig. 14 Normalized autocorrelation at the back lip location: cases 1, 2, 6, 7, and 9.

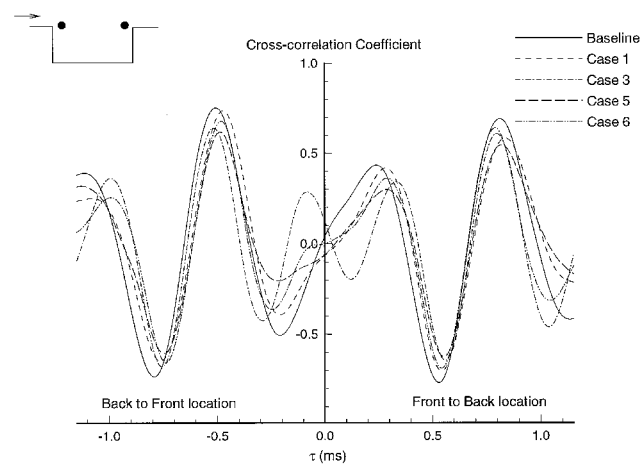

Fig. 15 Cross-correlation coefficient between front and back lip locations: cases 1, 3, 5, and 6.

at 0.2 ms is spurious and has no physical meaning. The true time lag for a disturbance convected from the front lip to the back lip is the peak at 0.83 ms; this corresponds to a speed 46% of the freestream speed. The time lag of the upstream propagating wave is −0.51 ms, which corresponds to a wave traveling at the speed of sound based on the cavity stagnation temperature. The cross-correlation amplitude for all of the cases shown has been slightly reduced, with the sinusoidal case, case 5, having the weakest correlation for both upstream and downstream propagating waves. The blowing, however, does not have a significant effect on the time lags.

Conclusions

The feasibility of using jet blowing to reduce the pressure oscillations in a compressible cavity flow has been examined using two-dimensional, time-accurate Navier–Stokes simulations. A small jet, placed within the cavity just below the front lip, was used to force the cavity shear layer. The forcing was found to be effective in reducing the large pressure oscillations, which are characteristic of open cavities. The effectiveness of the suppression was found to strongly depend on the amplitude and frequency of the jet and weakly depend on the phase angle and duty cycle of the jet. Autocorrelation analysis shows that the size of the vortical structures in the shear layer are reduced, and this may explain the reduction in the pressure amplitude of the oscillations. However, the cross-correlation analyses suggests that the timing of events within the cavity are unaffected by the jet blowing.

Acknowledgment

This work was conducted on the North Carolina Supercomputing Center's Cray Y-MP. The authors gratefully acknowledge this support.

References

[1]Shaw, L., Clark, R., and Talmadge, D., "F-111 Generic Weapons Bay Acoustic Environment," AIAA Paper 87-0168, Jan. 1987.

[2]Bliss, D. B., and Hayden, R. E., "Landing Gear and Cavity Noise Prediction," NASA CR-2714, July 1976.

[3]Roshko, A., "Some Measurements of Flow in a Rectangular Cutout," NACA TN 3488, Aug. 1955.

[4]Tam, C. K., and Block, P. J., "On the Tones and Pressure Oscillations Induced by Flow over Rectangular Cavities," *Journal of Fluid Mechanics*, Vol. 89, Pt. 2, 1978, pp. 373–399.

[5]Heller, H. H., and Bliss, D. B., "The Physical Mechanism of Flow-Induced Pressure Fluctuations in Cavities and Concepts for Their Suppression," AIAA Paper 75-491, March 1975.

[6]Rossiter, J. E., "Wind-Tunnel Experiments on the Flow over Rectangular Cavities at Subsonic and Transonic Speeds," NASA Ames Research Center, R&M 3438, Oct. 1964.

[7]Baysal, O., Yen, G., and Fouladi, K., "Navier-Stokes Computations of Cavity Aeroacoustics with Suppression Devices," *Journal of Vibrations and Acoustics*, Vol. 116, Jan. 1994, pp. 105–112.

[8]Chokani, N., and Kim, I., "Suppression of Pressure Oscillations in an Open Cavity by Passive Pneumatic Control," AIAA Paper 91-1729, June 1991.

[9]Vakili, A. D., Wolfe, R., Nagel, T., and Lambert, E., "Active Control of Cavity Aeroacoustics in High Speed Flows," AIAA Paper 95-0678, Jan. 1995.

[10]Sarno, R. L., and Franke, M. E., "Suppression of Flow-Induced Pressure Oscillations in Cavities," *Journal of Aircraft*, Vol. 31, No. 1, 1994, pp. 90–96.

[11]Morgenstern, A., Jr., and Chokani, N., "Hypersonic Flow Past Open Cavities," *AIAA Journal*, Vol. 32, No. 12, 1994, pp. 2387–2393.

[12]Morgenstern, A., "Numerical Investigation of Unsteady Hypersonic Flows Past Cavities," Ph.D. Dissertation, Mechanical and Aerospace Engineering Dept., North Carolina State Univ., Raleigh, NC, 1994.

[13]East, L. F., "Aerodynamically Induced Resonance in Rectangular Cavities," *Journal of Sound and Vibration*, Vol. 3, May 1966, pp. 277–287.

[14]Rizzetta, D. P., "Numerical Simulation of Supersonic Flow over a Three-Dimensional Cavity," *AIAA Journal*, Vol. 26, No. 7, 1988, pp. 799–807.

[15]Lamp, A., "Active Control of Cavity Flows by Using a Small Jet," M.S. Thesis, Mechanical and Aerospace Engineering Dept., North Carolina State Univ., Raleigh, NC, 1996.

[16]Burg, J., "Maximum Entropy Spectral Analysis," Ph.D. Dissertation, Stanford Univ., Stanford, CA, 1975.

[17]Heller, H. H., Holmes, D. G., and Covert, E. E., "Flow Induced Pressure Oscillations in Shallow Cavities," *Journal of Sound and Vibration*, Vol. 18, April 1971, pp. 545–553.